

The semiflexible fully-packed loop model and interacting rhombus tilings

Jesper Lykke Jacobsen¹ and Fabien Alet^{2,3}

¹Laboratoire de Physique Théorique de l'École Normale Supérieure, 24 rue Lhomond, 75231 Paris, France.

²Laboratoire de Physique Théorique, Université de Toulouse, UPS, (IRSAMC), F-31062 Toulouse, France

³CNRS, LPT (IRSAMC), F-31062 Toulouse, France

Motivated by a recent adsorption experiment [M.O. Blunt *et al.*, *Science* **322**, 1077 (2008)], we study tilings of the plane with three different types of rhombi. An interaction disfavors pairs of adjacent rhombi of the same type. This is shown to be a special case of a model of fully-packed loops with interactions between monomers at distance two along a loop. We solve the latter model using Coulomb gas techniques and show that its critical exponents vary continuously with the interaction strength. At low temperature it undergoes a Kosterlitz-Thouless transition to an ordered phase, which is predicted from numerics to occur at a temperature $T \sim 110K$ in the experiments.

Byzantine artists were probably the first to appreciate the beauty of tiling the plane with various types of polygons. Nowadays, random tilings are a major subject in mathematics and theoretical physics, with many applications to real condensed matter systems.

In a very recent experiment, Blunt *et al.* [1] study the adsorption of certain rod-like organic molecules (paraterphenyl-3,5,3',5'-tetracarboxylic acid) on a graphite substrate by scanning tunneling microscopy (STM). An idealization of the resulting pattern is shown in Fig. 1A. The rod-like molecules (shown as thick white lines) arrange as a dimer covering of the hexagonal lattice, and interact with their neighbors via hydrogen bonding of carboxylic acid groups (thick black lines). The bisectors of the latter define a rhombus tiling with three different types of rhombi. By image processing the STM pictures, large tiling configurations could be produced [1], with only $\sim 10^{-3}$ defects per molecule at room temperature.

Dimer coverings of various planar lattices have been well studied theoretically and the corresponding partition functions and various correlation functions have

been obtained exactly [2, 3]. Long-distance behavior is conveniently analysed in terms of an equivalent height model. For the hexagonal-lattice case, this is obtained [3] by defining a height difference ± 1 to each displacement along the junction between two rhombi, using the rule in Fig. 1B. In the continuum limit, one expects [3, 4] the height to behave as a Gaussian free field with some coupling g which can be computed exactly [2, 3].

The experimentally measured value of g [1] is however 1.66(8) times larger than the theoretical prediction. This discrepancy is attributed to interactions between pairs of neighboring dimers, with an energy penalty $\Delta E > 0$ for a parallel arrangement. This motivates the study of interacting rhombus tilings (IRT), where each tile junction carries a weight $w = e^{-\Delta E/T}$ (respectively 1) if it separates rhombi of identical (resp. different) types.

The purpose of this Letter is to study a more general model which contains the IRT as a special case. We define a *link* to be any edge of the hexagonal lattice *not* covered by a dimer. In Fig. 1A links are shown as thick black lines. With appropriate boundary conditions, the links form fully-packed loops, *i.e.* loops which jointly visit each of the lattice vertices once. Assign a weight n to each loop. Since each link \mathcal{L}_0 is a bisector of a tile junction, the weight w must be attributed to \mathcal{L}_0 if and only if the two links touching either end of \mathcal{L}_0 are parallel. This defines the partition function of the semiflexible fully-packed loop (SFPL) model:

$$Z_{\text{SFPLM}} = \sum_{\text{loops}} n^N w^{N_{\parallel}}. \quad (1)$$

When $n = 1$ we recover the IRT.

Below we solve the SFPL model in the critical regime $-2 < n \leq 2$ using Coulomb gas methods [4, 5]. The case $w = 1$ was previously shown [5] to be described by two free fields. We shall see that the interaction w changes the coupling g_1 of one of these fields, leaving the other g_2 unchanged. The ratio $\gamma = g_1/g_2$ is a non-universal decreasing function of w . We compute all critical exponents as functions of n and γ . When w becomes smaller than some critical w_c , the SFPL model undergoes a Kosterlitz-Thouless (KT) transition to an ordered,

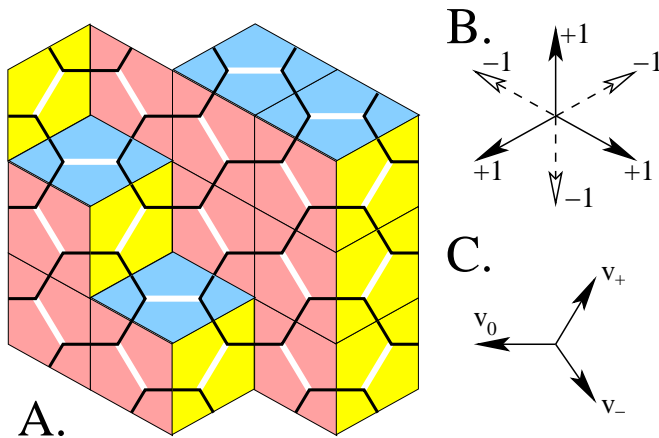


FIG. 1: (color online) Dimer covering of the hexagonal lattice (thick white lines), the complementary fully-packed loops (thick black lines), and corresponding rhombus tiling of the plane (A). Height mapping for the rhombus tilings (B) and for the fully-packed loop model (C).

non-critical state. Below we compute analytically the corresponding value of γ_c , and perform numerical simulations to compute the curve $\gamma(w)$. This allows to predict the value of the temperature at which the KT transition should occur in the experiments. We conclude the Letter by a critical discussion of the experimental realization [1], and a comparison with other related loop models.

2D height mapping. We briefly review the construction of Refs. [5, 6] and show how elements must be modified to account for the interaction w in the SFPL model.

Orient each loop independently and assign a weight $e^{-i\pi\epsilon_0}$ to clockwise and $e^{i\pi\epsilon_0}$ to counterclockwise loops. Parametrizing $n = 2 \cos(\pi\epsilon_0)$ we recover the correct loop weight after summing over orientations. Note that this is tantamount to a weight $e^{\pm i\pi\epsilon_0/6}$ to each left (resp. right) turn. Assign a label v_0 to edges covered by a dimer, and v_{\pm} to edges covered by a link going out of (resp. into) a vertex in the even sublattice. Each vertex is then adjacent to three edges, all carrying different labels (v_0, v_+, v_-) . Define the corresponding two-dimensional vectors $\mathbf{v}_0 = (-2, 0)$ and $\mathbf{v}_{\pm} = (1, \pm\sqrt{3})$ (see Fig. 1C). Attribute 2D heights $\mathbf{h} = (h^1, h^2)$ to the dual triangular lattice, by increasing \mathbf{h} by \mathbf{v}_i upon traversing an edge with label i . The traversal must be such that an even (resp. odd) vertex is seen on one's left (resp. right). The first component h^1 is precisely the 1D height defined by Fig. 1B for the rhombus tiling. Being complementary to loops with no orientation, the rhombi cannot “see” h^2 .

Coulomb gas approach. The partition function is written as a functional integral

$$Z = \int \mathcal{D}\mathbf{h}(\mathbf{x}) \exp(-S[\mathbf{h}(\mathbf{x})]), \quad (2)$$

where, by an abuse of notation, $\mathbf{h}(\mathbf{x})$ denotes the continuum limit of the height defined above, and the Euclidian action consists of three terms, $S = S_E + S_B + S_L$. The elastic term S_E is constrained by rotational invariance to take the form [with summation over repeated indices] $S_E = 1/2 \int d^2\mathbf{x} g_{\alpha\beta} \partial h^\alpha \cdot \partial h^\beta$, where $\partial = (\partial_1, \partial_2)$ is the usual gradient. The $D = 2$ -dimensional symmetric tensor $g_{\alpha\beta}$ is further constrained by symmetries. First, since loop orientations are eventually summed over, the action must be invariant under $v_+ \rightarrow v_-$, viz., $(h^1, h^2) \rightarrow (h^1, -h^2)$, implying $g_{12} = 0$. We denote henceforth $g_1 \equiv g_{11}$ and $g_2 \equiv g_{22}$. Second, a cyclic permutation of (v_0, v_+, v_-) maintains the chirality of the loop turns at each vertex, and is thus a symmetry for $w = 1$. This implies $g_1 = g_2$ in this case [5].

However, the cyclic permutation is *not* a symmetry of the SFPL model for $w \neq 1$. To see this, we inspect all possible configurations of the pair of vertices surrounding a fixed edge \mathcal{E}_0 . By rotation symmetry we can take \mathcal{E}_0 horizontal with an even vertex on its left end. By reflection symmetry it suffices to inspect six out of twelve configurations. This gives two groups of three configurations related by the cyclic permutation. As seen from

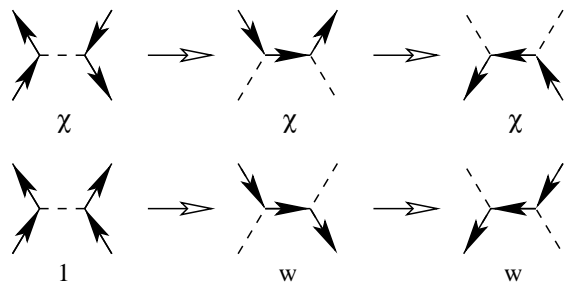


FIG. 2: The upper group of three configurations for a vertex pair has weights $\chi \equiv e^{i\pi\epsilon_0/3}$ which are invariant under the cyclic permutation of labels (v_0, v_+, v_-) , whereas the weights of the lower group differ by factors of w .

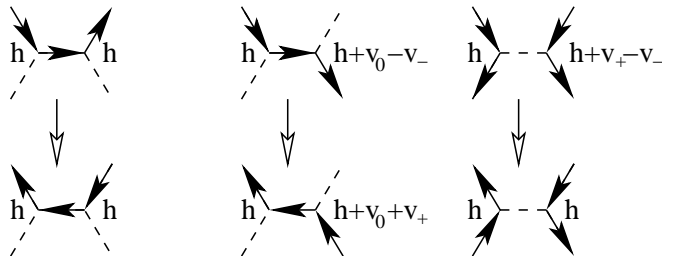


FIG. 3: Each column shows a pair of configurations with identical link positions, but different loop orientations. The middle column comes with a weight w .

Fig. 2 the members of the second group differ by factors of w , proving the statement. We now argue that changing the weight w will modify g_1 but leave g_2 unchanged. To this end, we consider pairs of local configurations having identical link positions, but which differ by the loop orientation. In Fig. 3 we show three such pairs (all others can be found by reflection and rotation) and evaluate the height gradient along the middle edge. In all cases, the w interaction must not distinguish between two members of a pair. We conclude that w must not couple to $\mathbf{v}_+ - \mathbf{v}_- = (0, 2\sqrt{3})$, which is proportional to h^2 . Conversely, configurations in the middle column of Fig. 3 have weight w and are the only ones to have a height gradient along $\mathbf{v}_0 \propto h^1$. This proves the claim.

The action also contains a boundary term $S_B = i/(4\pi) \int d^2\mathbf{x} (\mathbf{e}_0 \cdot \mathbf{h}) \mathcal{R}(\mathbf{x})$ where \mathcal{R} is the scalar curvature. The background electric charge \mathbf{e}_0 is easily computed on the cylinder, where it ensures the correct weighting of non-contractible loops. We have $\mathbf{e}_0 \cdot \mathbf{v}_0 = 0$ and $\mathbf{e}_0 \cdot \mathbf{v}_{\pm} = \pm\pi\epsilon_0$, implying $\mathbf{e}_0 = (0, \pi\epsilon_0/\sqrt{3})$.

Finally, the Liouville term S_L is the continuum limit of the local vertex weights. The height is compactified [5] with respect to a triangular lattice \mathcal{M} of side $2\sqrt{3}$ spanned by $\mathbf{v}_{\pm} - \mathbf{v}_0$. We can therefore expand S_L as a Fourier series over the vertex operators $e^{i\mathbf{e} \cdot \mathbf{h}}$, where the electric charges \mathbf{e} belong to the lattice \mathcal{E} reciprocal to \mathcal{M} . It suffices to keep the most relevant term which has the same periodicity as the vertex weights. The inclusion of

w does *not* change this periodicity, so we have $S_L \sim e^{i\mathbf{e}_s \cdot \mathbf{h}}$ where the screening charge reads $\mathbf{e}_s = (0, 2\pi/\sqrt{3})$.

Critical exponents. The critical exponent of an operator $\mathcal{O}_{\mathbf{e}, \mathbf{m}}$ with electric charge $\mathbf{e} \in \mathcal{E}$ and magnetic charge $\mathbf{m} \in \mathcal{M}$ reads [6, 7]:

$$x_{\mathbf{e}, \mathbf{m}} = [e_\alpha(e_\alpha - 2e_{0\alpha})/g_\alpha + g_\alpha m_\alpha^2]/(4\pi). \quad (3)$$

The corresponding two-point functions decay with distance r as $r^{-2x_{\mathbf{e}, \mathbf{m}}}$. To keep the model critical we impose [6] the exact marginality of S_L , whence $x_{\mathbf{e}_s, \mathbf{0}} = 2$, or

$$g_2 = (1 - e_0)\pi/6. \quad (4)$$

The other coupling g_1 depends non-universally on the microscopic weight w . Henceforth, we express everything in terms of e_0 and the ratio $\gamma \equiv g_1/g_2$. Note that $\gamma(w)$ is monotonically decreasing, and $\gamma(1) = 1$. Computing the actual function $\gamma(w)$ would require an exact solution, but it is doubtful that the SFPL model is integrable. Below, we perform numerical simulations to obtain this curve in the $n = 1$ case relevant to experiments.

The central charge is determined from the background electric charge as $c = 2 + 12x_{\mathbf{e}_0, \mathbf{0}} = 2 - 6e_0^2/(1 - e_0)$, independent of γ .

An important class of critical exponents is the so-called watermelon exponents x_k . They measure the probability of having k oriented loop strands emanating from some small neighborhood (of size a a few lattice constants) and absorbed by some other neighborhood at distance $r \gg 1$. The corresponding height defect (vortex) has magnetic charge \mathbf{m}_k which is computed by noting that $\mathbf{v}_+ - \mathbf{v}_-$ generates a pair of strands, and $2\mathbf{v}_0 - \mathbf{v}_+$ generates a single strand [5]. Setting $\delta_k = k \bmod 2 \in \{0, 1\}$ we find explicitly $\mathbf{m}_k = (-3\delta_k, \sqrt{3}k)$. This leads to

$$x_k = x_{\mathbf{e}_0, \mathbf{m}_k} = (k^2 + 3\gamma\delta_k)(1 - e_0)/8 - e_0^2/(2 - 2e_0). \quad (5)$$

Another type of vortex corresponds to having a vertex not visited by any loop. The corresponding magnetic charge is $\mathbf{m}_T = 3\mathbf{v}_0 = (-6, 0)$, and the exponent

$$x_T = x_{\mathbf{0}, \mathbf{m}_T} = 3\gamma(1 - e_0)/2. \quad (6)$$

In the IRT model, the second height component is “invisible” and only x_1 and x_T are meaningful. In the tiling picture, the corresponding defects are compounds of three (resp. four) elementary triangles forming a trapezoid (resp. triangle) of base length two. Since $e_0 = 1/3$, we have $g_2 = \pi/9$, $c = 1$, $x_1 = \gamma/4$ and $x_T = \gamma$.

Kosterlitz-Thouless transition. Due to the compactification, any functional of the heights can be expanded over vertex operators with charges in \mathcal{E} , a triangular lattice of side $2\pi/3$. The crucial step in solving the SFPL model was to fix the coupling by requiring the exact marginality of S_L . By examining the symmetries of local vertex weights, one finds [5] that vertex operators appearing in the expansion of S_L have charges in a sublattice

$\mathcal{E}_L \subset \mathcal{E}$, a triangular lattice of side $2\pi/\sqrt{3}$ spanned by the second-shortest vectors in \mathcal{E} . For $e_0 > 0$, the most relevant vertex operator has $\mathbf{e} = \mathbf{e}_s = (0, 2\pi/\sqrt{3})$, and the solution Eq. (4) was obtained by using this as the screening charge, *i.e.* by setting $x_{\mathbf{e}_s, \mathbf{0}} = 2$.

One can add another term S_F to the action that favors domains where the height interface is locally flat. Its vertex operators have charges in a sublattice $\mathcal{E}_F \subset \mathcal{E}_L$, a triangular lattice of side 2π spanned by the second-shortest vectors in \mathcal{E}_L . The interface is in a rough, critical (resp. smooth, non-critical) phase when S_F is irrelevant (resp. relevant). Increasing γ beyond a certain critical value $\gamma_c > 1$ induces a KT transition to the smooth phase. The most relevant vertex operator in S_F has $\mathbf{e}_F = (\pm 2\pi, 0)$. We can find γ_c by setting $x_{\mathbf{e}_F, \mathbf{0}} = 2$, yielding

$$\gamma_c = (1 - e_0)/3. \quad (7)$$

In the non-critical phase, the couplings g_1 and g_2 will renormalize to infinity, corresponding to a microscopic parameter $w \rightarrow 0$. The situation $w = 0$ corresponds in Fig. 1A to the links forming small loops of length six around one of the three sublattices (denoted \mathcal{L}_a with $a = 1, 2, 3$) of the triangular lattice. Which sublattice is selected is a matter of spontaneous symmetry breaking. Equivalently, in the rhombus picture, the average number of rhombi N_a touching a vertex of \mathcal{L}_a will saturate to $(N_1, N_2, N_3) = (6, 3, 3)$ or any permutation thereof.

The exact exponents at the KT transition are found by inserting Eq. (7) into Eqs. (5) and (6). Note in particular that $x_T(\gamma_c) = 9/2$ is independent of e_0 .

Experimental realization. As mentioned in the introduction, a handsome experimental realization of the IRT model appeared recently [1]. The energy scales of the experiment are such that, once formed, the tilings are static (but certain defects can move around dynamically; see below). Statistics on the height fluctuations can however be obtained by taking STM pictures of various regions. These fluctuations were reported to be critical [1], and an experimental value $\gamma_{\text{exp}} = 1.66 \pm 0.08$ was observed. Since $\gamma_{\text{exp}} < \gamma_c$ with $\gamma_c = 9/2$ in the $e_0 = 1/3$ IRT case, our analysis confirms that the system is indeed critical.

To fix the experimental energy scales within the IRT model, we perform numerical simulations with Transfer Matrix (TM) and Monte Carlo (MC) techniques similar to those developed in Ref. [8]. Fig. 4A shows c as a function of w , as determined from the TM calculations. A clear $c = 1$ plateau appears, corresponding to the critical phase for $w > w_c$. We also measured γ from the determination of x_1 in TM simulations and winding number fluctuations in MC simulations [8, 9]. The resulting $\gamma(w)$ curve is displayed in Fig. 4B. Extrapolations of w_c to the thermodynamic limit are made: (A) from the TM data by studying the intersections $c = 1$ and $\gamma_c = 9/2$, giving $w_c = 0.635(2)$ in both cases, and (B) from the MC data by studying order parameter fluctuations, giving $w_c = 0.640(5)$. We also find that the experimental

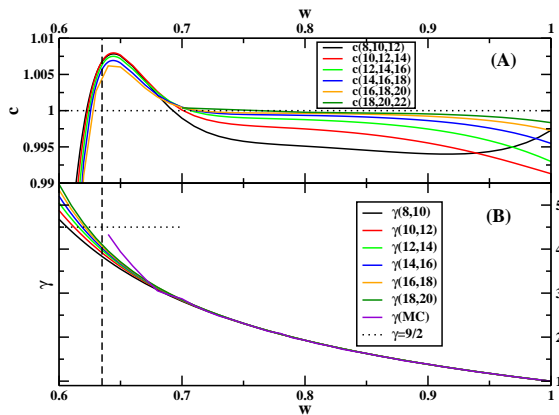


FIG. 4: (color online) Numerical simulations of the IRT model. As functions of w : (A) Central charge c , obtained from three-point fits of the free energy on cylinders of circumference L . (B) Coupling constant ratio γ , found from two-point fits for the critical exponent x_1 (TM data), and from winding number fluctuations on a 768×256 sample (MC data). The long-dashed vertical line denotes $w_c = 0.635$.

value $\gamma_{\text{exp}} = 1.66(8)$ corresponds to $w_{\text{exp}} = 0.845(15)$, allowing to determine the energy scale of nearest-neighbor interactions as $\Delta E \simeq 4.25\text{meV}$. We therefore predict the KT transition to occur at $T = T_c \simeq 110\text{K}$ in the experimental compound. The transition could be observed by monitoring γ_{exp} up to the temperature where it takes the value γ_c , as in Ref. 10. For the precise compound of Ref. [1], this will require performing the experiment in vacuum, to avoid that the solvent freezes [11].

Among the two possible topological defects \mathbf{m}_1 and \mathbf{m}_T in the IRT model, the former is by far the most probable, since $x_T = 4x_1 (= \gamma)$. Defects of the \mathbf{m}_T type, if observable, would indeed be very closely bound. In the dimer language, the \mathbf{m}_1 defect can correspond either to zero or two dimers incident to the same vertex. Both possibilities were observed in the STM scans, although the latter was dismissed as a transient image artifact (see in particular Fig. 3E of Ref. [1]). The dynamics of defect pairs should make it experimentally possible to gather statistics on their relative separation r . Given γ_{exp} , the above theory predicts the corresponding power law.

Discussion. We have solved a model of semiflexible fully-packed loops, and shown that the bending rigidity couples to just one of the two coupling constants in the equivalent 2D height model. Although we have here given a microscopic argument that only g_1 was affected, it should be noted that this is also a consequence of the

field theory. Indeed, since the screening charge \mathbf{e}_s is in the h^2 direction, g_2 is in fact bound to renormalize to the universal value Eq. (4). The field theory should remain valid for other microscopic interactions that have the effect of rendering the height interface stiffer.

The particular case of interacting random tilings obtained when $n = 1$ has a physics similar to that of dimer coverings of the *square* lattice with local aligning interactions [8]. The SFPL model can also be compared to the 3D height construction used in Ref. [12] to solve the Flory model of protein melting.

Adding a *finite* density of \mathbf{m}_T type defects to the SFPL model induces a flow towards the well-known dense phase of the $O(n)$ model [13]. Starting from the 2D height mapping, the h^1 component now becomes massive, and the dense phase is described by h^2 . Since the corresponding coupling g_2 is insensitive to w , we deduce that bending rigidity is irrelevant in the dense $O(n)$ model and merely renormalizes the effective monomer length.

Note added. Another experimental realization of the IRT model has appeared very recently [14].

We thank the European Community Network ENRAGE (grant MRTN-CT-2004-005616) and the Agence Nationale de la Recherche (grant ANR-06-BLAN-0124-03) for support.

-
- [1] M.O. Blunt *et al.*, Science **322**, 1077 (2008).
 - [2] P.W. Kasteleyn, J. Math. Phys. **4**, 287 (1963); M.E. Fisher, Phys. Rev. **124**, 1664 (1961); M.E. Fisher and J. Stephenson, *ibid.* **132**, 1411 (1963).
 - [3] H.W.J. Blöte and H.J. Hilhorst, J. Phys. A **15**, L631 (1982).
 - [4] B. Nienhuis, J. Stat. Phys. **34**, 731 (1984).
 - [5] J. Kondev, J. de Gier and B. Nienhuis, J. Phys. A **29**, 6489 (1996).
 - [6] J.L. Jacobsen and J. Kondev, Nucl. Phys. B **532**, 635 (1998).
 - [7] V.I.S. Dotsenko and V.A. Fateev, Nucl. Phys. B **240**, 312 (1984).
 - [8] F. Alet *et al.*, Phys. Rev. Lett. **94**, 235702 (2005); Phys. Rev. E **74**, 041124 (2006).
 - [9] C. Boutillier and B. de Tilière, preprint math/0608600.
 - [10] M.S. Hoogeman *et al.*, Phys. Rev. Lett. **82**, 1728 (1999)
 - [11] P. Beton, private communication.
 - [12] J.L. Jacobsen and J. Kondev, Phys. Rev. Lett. **92**, 210601 (2004); Phys. Rev. E **69**, 066108 (2004).
 - [13] B. Nienhuis, Phys. Rev. Lett. **49**, 1062 (1982).
 - [14] Y. Han *et al.*, Nature **456**, 898 (2008).